GCN5 negatively regulates class III peroxidases PRX71 and PRX33 to promote lignin deposition in Arabidopsis

Mansi Sharma, Jan Masood, Pavel Kerchev, Iva Mozgova, Michael Wrzaczek

[1]Institute of Plant Molecular Biology, Biology Centre, Czech Academy of Sciences, 37005 České Budějovice, Czech Republic

[2]Faculty of Science, University of South Bohemia, 37005 České Budějovice, Czech Republic

[3]Mendel University in Brno, 613 00 Brno, Czech Republic

[4]Horticultural Sciences Department, University of Florida, Gainesville, FL, USA, 32611

[5]Current address: Estación Experimental del Zaidín (EEZ-CSIC), 18008, Granada, Spain

[*]Corresponding author: Michael Wrzaczek (michael.wrzaczek@umbr.cas.cz)

Abstract

Histone acetylation shapes transcriptional programs during environmental stress. The Arabidopsis histone acetyltransferase *GCN5* (*HAG1*), a catalytic subunit of the SAGA complex, has been implicated in salt stress responses and cell wall integrity. Here, we show that loss of *GCN5* enhances reactive oxygen species (ROS) accumulation and is accompanied by altered expression of class III peroxidase genes, with strong salt-induced upregulation of PRX71 and elevated basal PRX33 transcript abundance. Consistent with a role for these peroxidases in stress-associated cell wall remodeling, overexpression of *PRX71* or *PRX33* in the wild type is sufficient to promote ectopic lignin deposition in roots. Conversely, *prx71* and prx33 mutants show improved growth on salt and on the cellulose biosynthesis inhibitor isoxaben, and they lack the pronounced ectopic root lignification observed in gcn5 under salt stress. Chromatin immunoprecipitation followed by qPCR (ChIP-qPCR) reveals reduced H3K9 acetylation at *PRX71* and *PRX33* promoter regions in *gcn5* compared with the wild type, and reduced transcript abundance of candidate transcription factors (TFs), including MYBS2 and GATA21, accompanied by reduced H3K9ac at their loci. Together, our results support a model in which GCN5 constrains *PRX71/PRX33*-mediated lignification during stress, likely through an indirect regulatory route that integrates chromatin state and transcription factor activity to limit stress-associated lignification while maintaining root growth under salt stress.

Keywords

Arabidopsis thaliana; *GCN5/HAG1*; histone acetylation; H3K9ac; salt stress; cell wall integrity; lignification; class III peroxidase; reactive oxygen species

Introduction

Plants are constantly exposed to abiotic and biotic stresses that can occur alone or in combination, requiring rapid signaling as well as longer-term acclimation (Boudsocq & Sheen, 2013; Wurzinger et al., 2011). Among the earliest responses are changes in cytosolic calcium levels and the production of reactive oxygen species (ROS), which act as signaling molecules (Boudsocq & Sheen, 2013; Wurzinger et al., 2011). Stress also activates mitogen-activated protein kinase (MAPK) activation and hormone signaling networks (Baxter et al., 2014; Jalmi & Sinha, 2015; Mittler, 2002; Xia et al., 2015). Among these stresses, salt stress is a major abiotic constraint because it imposes an early osmotic limitation on growth and a later ionic phase that can exacerbate cellular damage (Munns & Tester, 2008). Plants rapidly respond to biotic and abiotic stimuli by triggering responses that involve changes to gene transcription, inherently connected to changes in chromatin structure, and can also orchestrate rapid but long-lasting epigenetic changes in response to stress. These changes including histone modifications, are inducible within minutes to hours but can persist for days after the initial stimulus and gradually fade, depending on the locus and stress regime (Ding et al., 2012; Lämke & Bäurle, 2017; Ma et al., 2025). Chromatin structure is determined by combinations of histone modifications—including acetylation, methylation, phosphorylation, ubiquitylation, and sumoylation as well as by DNA methylation, which regulate gene expression without altering the DNA sequence.

Among these modifications, histone acetylation plays a key role in modulating chromatin accessibility. Histone acetylation status is balanced by the activities of histone acetyltransferases (HATs) and histone deacetylases (HDACs), and can be modulated under stress conditions (Ueda & Seki, 2020). This balance can be altered, for example, treatment with the HDAC inhibitor Ky-2 increases histone acetylation in *Arabidopsis thaliana* under salt stress, leading to increased expression of salt-responsive genes and contributing to improved salt tolerance (Sako et al., 2016). One well characterized HAT module involved in histone acetylation includes General control non-repressed protein 5 (GCN5), along with Alteration/Deficiency in Activation 2B(ADA2B), Alteration/Deficiency in Activation 3 (ADA3), SGF29 (SAGA-associated factor 29) subunits (Moraga & Aquea, 2015). GCN5 acetylates specific lysines on histone H3 at position K9, K14, K27, and histone H4 at position K12, and is crucial for regulating the expression of genes involved in plant development and stress responses (Benhamed et al., 2006; Hu et al., 2015; Kim et al., 2020; Servet et al., 2010; Zheng et al., 2019).

Importantly, GCN5 functions as a part of the SAGA (Spt–Ada–Gcn5 acetyltransferase) complex, a conserved transcriptional coactivation protein complex in eukaryotes, that influences a wide range of cellular processes by modulating histones through acetylation and deubiquitination (Moraga & Aquea, 2015). Furthermore, GCN5 is involved in salt stress tolerance and cell-wall integrity by modulating H3K9 and H3K14 acetylation, a modification linked to the activation of

chitinase-like-1 (CTL1), polygalacturonase involved in expansion-3 (PGX3), and MYB domain protein54 (MYB54) genes associated with cellulose synthesis, thereby changing turgor, growth dynamics, and wall integrity, and plants actively remodel wall polymers to maintain growth and survival (Zheng et al., 2019).

In addition to the SAGA complex, plants have been recently proposed to also contain a PAGA (Plant-ADA2A-GCN5-acetyltransferase) complex, which contributes to the regulation of transcription of hormone-related genes that control plant growth traits such as height and branching. While SAGA complex contains the GCN5 subunit together with ADA2B, both SAGA and PAGA share the GCN5 subunit, which regulates histone acetylation, and the two complexes independently generate different levels of acetylation, thereby facilitating transcriptional activation (Wu et al., 2023).

A key aspect of plant growth and environmental response is the continuous modification of the cell wall, which is loosened to enable cell expansion and serves as the plant's first line of defense against stress during pathogen attack and osmotic or salt stress, requiring remodeling to maintain integrity and prevent collapse (Cosgrove, 2016; Tenhaken, 2015). s The plant cell wall consists of hemicellulose, pectin, and cellulose, which is a primary and essential polysaccharide composed of long, unbranched chains of β-1,4-linked glucose units (Somerville et al., 2004), with cellulose synthesized by cellulose synthase (CESA) proteins (Cosgrove, 2005; Gutierrez et al., 2009). Loss of function or chemical inhibition of CESA such as by isoxaben or thaxtomin□A, disrupts cellulose biosynthesis and cell wall integrity, which results in ectopic lignin deposition (Bischoff et al., 2009; Caño□Delgado et al., 2003; Persson et al., 2007). In addition to its ectopic deposition under stress, lignin is normally deposited in the secondary cell wall, strengthening the tissue and making the wall less permeable to water and facilitating water transport through the xylem (Boyce et al., 2004; Rogers & Campbell, 2004). Abiotic and biotic stresses can modulate the expression of lignin biosynthesis genes including in *Arabidopsis*, under salt stress, lignin accumulation is accompanied by higher expression of lignin biosynthesis genes (Chun et al., 2019; Moura et al., 2010). The stress induced lignin deposits occurs as a secondary cell wall remodeling response mediated by class III peroxidases (PRXs), which comprise 73 isoforms in *Arabidopsis* that use H□O□ to oxidize monolignols, leading to lignin formation (Bischoff et al., 2009; Marjamaa et al., 2009; Passardi et al., 2004). Specific *PRXs*, including *PRX2*, *PRX25*, and *PRX71*, contribute to stem lignification, with mutants showing reduced lignin without developmental defects (Shigeto et al., 2013). *PRX71* also plays a role in reinforcing the cell wall, which helps limit cell expansion, and is upregulated in plants with altered pectin or after cellulose synthesis inhibition, promoting ROS accumulation and influencing growth (Raggi et al., 2015), while knockdown of *PRX33* and *PRX34* reduces MAMP□induced defense proteins, lowers apoplastic ROS production and alters cell wall remodeling enzymes (Daudi et al., 2012; O'Brien et al., 2012). Together, these observations place peroxidase-driven ROS and lignification at the

intersection of stress signaling and cell wall remodeling. Yet, it remains unclear how the chromatin-level mechanisms tune PRX gene expression during salt stress.

Here, we investigate how GCN5 influences the expression of two class III peroxidases, *PRX71* and *PRX33*, and how this relates to ROS accumulation and lignin deposition during salt stress. Using genetic and transgenic lines, histochemical assays, gene expression profiling, and ChIP-qPCR, we identify an association between GCN5-dependent acetylation and a transcriptional network that constrains peroxidase-linked lignification in stressed seedlings. By connecting a chromatin regulator (GCN5) to distinct PRX loci and downstream cell wall phenotypes, this work aims to clarify how epigenetic control helps balance stress protection with growth in salt-challenged seedlings.

Results

Loss of GCN5 increases ROS accumulation and alters *PRX33* and *PRX71* expression during salt stress

To confirm and extend the previous reports that *gcn5* is sensitive to salt stress (Zheng et al., 2019), we analyzed the survival rate and root growth of *gcn5* seedlings under 150 mM NaCl. We included *gcn5* mutants, wild-type plants, and three independent complementation lines expressing *pGCN5::GCN5-GFP* in the *gcn5* mutant background (described in De Smet et al., 2025) to confirm that the observed phenotypes were specifically caused by the loss of GCN5. Survival rates and primary root lengths on 150 mM NaCl were measured on day 12 and normalized to control conditions (Figure S1a, b). The *gcn5* mutant showed reduced survival and shorter primary root length compared with wild type (survival rate, Figure S1a; root length, Figure S1b). All three complementation lines partially rescued the survival phenotype (Figure S1a) and restored root length to levels similar to the wild type (Figure S1b).

Consistent with previous findings (Zheng et al., 2019), we observed that the *gcn5* mutant was sensitive to salt stress. Salt stress induces ROS accumulation (Mittler, 2002) and GCN5 may play a role in maintaining ROS balance under salt stress. *TaHAG1*, a wheat ortholog of GCN5, contributes to ROS balance under salt stress (Zheng et al., 2021a). We next investigated whether loss of GCN5 affects ROS accumulation in *Arabidopsis.* To examine this, we performed DAB staining to visualize hydrogen peroxide accumulation in 10-day-old *gcn5* and wild type plants following 6 hours of treatment with 150 mM NaCl or 300 nM isoxaben. Isoxaben, which triggers a wide spectrum of cell wall integrity-related adaptations, including hormone signaling and lignin accumulation, by disrupting cellulose biosynthesis (Denness et al., 2011; Hamann, 2015; Scheible et al., 2001). We observed enhanced ROS accumulation in *gcn5* under mock conditions, whereas no ROS accumulation was detected in wild type plants. However, in response to NaCl and isoxaben treatments, we observed enhanced ROS accumulation in the *gcn5* mutant compared with wild type (Figure 1a).

To explore the molecular basis of the elevated ROS accumulation under control conditions, we analyzed publicly available transcriptomic data to identify differentially expressed genes in the

gcn5 mutant (Wu et al., 2023). This analysis revealed the 24 misregulated peroxidase genes in *gcn5* mutant, out of which 21 were upregulated and 3 downregulated (Figure S1c). Since the enhanced salt sensitivity of the *gcn5* plants was previously connected with altered cell wall synthesis and enhanced lignin deposition (Zheng et al., 2019), and we therefore focused on class III PRXs, given their roles in lignin polymerization (Cosio & Dunand, 2009). The upregulation of class III PRXs, in *gcn5* could influence ROS balance, as they utilize H_20_2 during lignin polymerization. We hypothesized that the increased expression of these *PRX* genes in the *gcn5* mutant contributes to lignin deposition, as lignin is known to accumulate in response to cell wall damage (Denness et al., 2011; Passardi et al., 2004).

Transcript abundance of five misregulated *PRX* genes, selected from transcriptional analysis was analyzed by qRT-PCR at different time points after treatment with 150 mM NaCl in wild type and *gcn5* (Figure S1d). Among them *PRX33* and *PRX71* showed consistently higher expression in *gcn5* compared to wild-type plants. *PRX33* was elevated in *gcn5* under control conditions but showed a weaker induction upon salt treatment compared to wild type. By contrast, *PRX71* transcript abundance increased after 6 hours of NaCl treatment and continued to rise up to 12 hours, reaching levels significantly higher than those in wild type (Figure 1b). Overall, this indicates that *PRX33* and *PRX71* are upregulated in the *gcn5* mutant and were therefore selected for subsequent functional analyses.

().

***PRX33* and *PRX71* overexpression alters lignin deposition**

To test whether this PRX upregulation is sufficient to drive the lignification phenotype, we next examined *PRX33* and *PRX71* gain-of-function lines. Based on our observation that loss of *GCN5* resulted in enhanced *PRX33* and *PRX71* expression and the involvement of class III *PRXs* in lignin polymerization, we next investigated whether upregulation of *PRX33* and *PRX71* in *gcn5* contributes to enhanced lignin deposition and potentially to maintaining cell wall integrity. To this end, we generated PRX overexpression lines in wild type background. To visualize lignin, we used phloroglucinol-HCl staining, which reacts with the aldehyde group of lignin and results in a pink coloration (Davidson et al., 1995; Pradhan Mitra & Loqué, 2014). Lignin deposition was examined in 2-week-old roots old under control conditions in wild type, *gcn5*, *prx71*, *prx33*, and PRX overexpression lines. The *gcn5* mutant displayed increased lignin deposition in the vasculature compared with wild type roots, whereas *prx71* and *prx33* resembled wild type roots. PRX overexpression lines showed enhanced lignin deposition in the vasculature, similar to *gcn5*, but also displayed ectopic lignin accumulation (Figure 2a). These results indicate that elevated PRX expression is sufficient to promote vascular and ectopic lignin deposition, recapitulating key aspects of the *gcn5* phenotype.

Given these observations and because GCN5 loss leads to reduced cellulose content, as it regulates cellulose synthesis genes (Zheng et al., 2019), increased lignin deposition could serve as a compensatory reinforcement mechanism to maintain cell wall strength. Consistent with this idea, our

findings indicate that *PRX33* and *PRX71* promote vascular and ectopic lignin deposition, which may help to counteract cell wall disruption.

Altered lignin deposition and reduced root growth in *gcn5* under salt stress

Considering the increased lignin deposition in both *gcn5* and PRX overexpression lines, we next asked how these changes relate to salt-driven root growth phenotypes. To understand the roles of *PRX71* and *PRX33* in response to salt stress, we analyzed salt sensitivity and root growth following salt stress and isoxaben treatment in the *prx71-1*, *prx71-2*, and *prx33* loss-of-function mutants, together with *gcn5* and wild-type plants. We included the *gcn5* complementation lines as a control to confirm that the *gcn5* phenotypes were specifically caused by loss of *GCN5*. Under NaCl stress, the *gcn5* mutant showed reduced survival compared with wild type plants, whereas the complementation lines showed higher survival than *gcn5*, partially rescuing the phenotype (Figure 3a, S2a). In contrast, the *prx71-1* and *prx33* mutants showed statistically higher survival than wild type plants, while *prx71-2* had survival levels similar to *prx71-1* and *prx33* (Figure 3a). To assess growth responses under cell wall stress, we analyzed root length under NaCl and isoxaben treatments (Figure 3b,c). Root lengths were normalized to control conditions (Figure S2b,c). The *prx71-1*, *prx71-2*, and *prx33* maintained significantly longer primary roots compared with wild type plants, whereas the three complementation lines exhibited root lengths similar to wild type (Figure 3b,c). In contrast, *gcn5* seedlings displayed strongly reduced root elongation under both stress conditions (Figure 3b,c).

We next examined lignin deposition in 10-day-old roots of *gcn5*, *prx71-1*, and *prx33* mutants in response to salt stress. The *gcn5* mutant showed increased lignin deposition after 6 hours of treatment with 150 mM NaCl, including enhanced accumulation in the vasculature and ectopic deposition. In wild type, lignin accumulation was also observed after 6 hours of treatment, whereas *prx71-1* and *prx33* mutants did not show detectable lignin. The absence of lignin deposition in *prx71-1* and *prx33* under salt stress suggests that these peroxidases are critical for lignin deposition during salt-induced cell wall stress (Figure 3d). Together, these results indicate that PRX71 and PRX33 are responsible for lignin deposition in response to salt stress. Furthermore, the absence of lignin deposition in *prx71-1* and *prx33* mutants correlates with increased root elongation under salt treatment, suggesting that lignin accumulation contributes to root growth restriction in response to stress-associated cell wall disruption.

Indirect regulation of *PRX71* and *PRX33* transcription by GCN5 through chromatin modification

Given this genetic link between GCN5, PRX function, and lignin deposition, we next examined whether GCN5 influences PRX33 and PRX71 transcription through chromatin modification. Since *PRX33* and *PRX71* were upregulated in the *gcn5* mutant (Figure 1b), although histone acetylation has

an activating effect on gene expression and loss of GCN5 results in reduced histone acetylation, we observed higher expression of *PRX33* and *PRX71* in the *gcn5* mutant. To investigate this further, we examined whether this may be reflected in the amount of histone acetylation at the gene loci, in particular the promoter regions. To examine this, we performed chromatin immunoprecipitation (ChIP) assays using an anti-H3K9ac antibody to analyze histone acetylation at the promoter regions of the *PRX71* and *PRX33* genes. Wild type and *gcn5* seedlings were grown on half-strength MS medium for 10 days, followed by treatment with 150 mM NaCl in liquid medium for 3 hours, control samples did not receive NaCl treatment. Samples were then collected for ChIP assay. The immunoprecipitated chromatin DNA was analyzed by qPCR to check enrichment levels relative to total H3 levels. In line with the histone acetyltransferase function of GCN5, the ChIP–qPCR analysis showed reduced H3K9ac enrichment at the promoter regions of *PRX71* and *PRX33* in the *gcn5* mutant compared with the wild type under both control and salt-stress conditions (Figure 4a, b). A transposable element locus, *At4g03770*, was used as a negative control to validate the ChIP–qPCR assay. (Figure 4c). Despite the decrease in H3K9ac at the *PRX33* and *PRX71* loci in *gcn5*, their expression tended to be elevated under control (*PRX33*) or NaCl-treated (*PRX71*) conditions (Figure 1b). This indicated that the upregulation of these genes in *gcn5* may be indirectly connected to the catalytic function of GCN5. Therefore, we explored potential transcriptional repressors involved in the regulation of these two *PRX* genes, hypothesizing that the absence of *gcn5* and resulting lower level of H3K9ac at a regulatory gene may promote (prime) the ready activation of *PRX33* and *PRX71*. Using publicly available transcriptomic data and ChIP-seq data, we searched for genes downregulated in *gcn5* that carry less H3K9ac in *gcn5* (Benhamed et al., 2008; Wu et al., 2023) and that have been identified as direct targets of GCN5 in wild type (Kim et al., 2020). Next, we analyzed potential transcription factor binding sites in the promoters of *PRX71* and *PRX33* using the Plant Promoter Analysis Navigator (PlantPAN) 4.0 (Chow et al., 2024), an online plant promoter analysis tool, and selected 16 transcription factors predicted to bind to one or both genes (Supplementary Table S2). We then compared the transcription factors predicted to bind the promoters of *PRX71* and *PRX33* with the list of *GCN5*-dependent genes identified from transcriptomic and ChIP-seq data.

This led to the identification of transcription factors that could potentially regulate (repress) the *PRX71* and *PRX33* genes in a *GCN5* -dependent manner. Next, we analyzed the transcript levels of the 16 TFs in wild type and *gcn5* seedlings under control conditions by qRT–PCR (Figure S3a) and identified 3 candidates that were differentially expressed in *gcn5* (Figure 4d, S3a). Among these candidates, GATA-type zinc finger transcription factor 21 (*GATA21*) were predicted to bind the promoters of both *PRX71* and *PRX33*, whereas MYB-related transcription factor 2 (*MYBS2*) and basic helix-loop-helix 137 (*BHLH137*) was predicted to bind only the PRX33 promoter. Of these, 2 transcription factors, GATA□type zinc finger transcription factor 21 (*GATA21)* and MYB□related transcription factor 2 (*MYBS2)* were downregulated in our experimental conditions, as expected in line with the requirement of GCN5 for their activation (Figure 4c). We next asked whether the

downregulation of these genes in *gcn5* is associated with the loss of H3K9ac In line with expectation, ChIP–qPCR analysis revealed lower enrichment of H3K9ac at the promoters of *MYBS2* and *GATA21* (Figure 4e, S3b). Together, these findings suggest that *GCN5* may influence *PRX71* and *PRX33* gene expression indirectly through transcription factors such as *MYBS2* and *GATA21*.

Discussion

GCN5 is a subunit of the histone acetyltransferase (HAT) module shared by the SAGA and PAGA complexes, where it facilitates histone acetylation, thereby contributing to the regulation of gene expression and numerous plant developmental pathways (Vlachonasios et al., 2003; Wu et al., 2023). Consistent with this central regulatory role, loss of *GCN5* function results in reduced plant size (Vlachonasios et al., 2003), short roots and defects in meristem activity (Kornet & Scheres, 2009; Servet et al., 2010) as well as other developmental defects, and is associated with altered expression of stress-responsive genes under various environmental stimuli, such as heat□induced *HSFA3* and *UVH6* (Benhamed et al., 2006; Hu et al., 2015). Taken together with our Results, these studies position GCN5 as a key coordinator of growth and stress adaptation, and our data extend this role to ROS homeostasis and PRX-dependent lignification during salt stress.

In response to salt stress, *TaHAG1*, the wheat ortholog of *Arabidopsis GCN5*, helps maintain ROS balance. In TaHAG1 overexpression lines, cytosolic antioxidant enzymes exhibit increased activity. However, it remains unclear whether this results from direct gene regulation by *TaHAG1* or from its effect on ROS-detoxifying pathways (Zheng et al., 2021b). In addition, a study in *Arabidopsis* has shown that GCN5 contributes to maintaining cell wall integrity under salt stress by influencing the expression of genes involved in cellulose synthesis. Compared with wild-type seedlings, *gcn5* mutants exhibit reduced cellulose content, which is further decreased under salt stress, while lignin accumulation is enhanced with ectopic lignification (Zheng et al., 2019). Our observations extend these findings by showing that under 150 mM NaCl stress, *gcn5* seedlings accumulate elevated levels of ROS and, interestingly shows altered expression of several class III *PRXs*. In particular, we identified *PRX33* and *PRX71* as the most promising candidates (Fig. 1a, b). Previous studies have shown that in *Arabidopsis*, Class III *PRXs* like *PRX71* limits root elongation (Raggi et al., 2015) and overexpression of *AtPRX37* leads to dwarf phenotypes (Pedreira et al., 2011), suggesting that altered peroxidase activity may contribute to root growth restriction in *gcn5*. In this framework, the elevated ROS and PRX mis-regulation we observe in *gcn5* provides a plausible route by which a chromatin-level perturbation can be translated into a cell-wall–centered growth phenotype under salt stress (Fig. 3b, c).

Lignin deposition has been reported in response to cell wall damage during stress conditions, which helps reinforce cell wall integrity (Caño□Delgado et al., 2003; Denness et al., 2011). Class III *PRXs* are centrally involved in controlling lignin deposition (Cosio & Dunand, 2009; Marjamaa et al.,

2009). Lignin deposition in response to salt stress has been reported in multiple plant species, including maize, where secondary cell wall lignin increases (Oliveira et al., 2020) and in *Arabidopsis*, showing elevated lignin accumulation (Chun et al., 2019). We observed that both *35S::PRX71* and *35S::PRX33* lines exhibit lignin accumulation comparable to the *gcn5* mutant under control conditions. Overall, the data support a role for *PRX33* and *PRX71* in mediating lignification as part of the cell-wall reinforcement response when cell-wall integrity is compromised. A parsimonious interpretation of our Results is that loss of *GCN5* shifts the balance toward ROS accumulation and PRX-associated lignification (Fig. 1a; Fig. 2a; Fig. 3d), and this enhanced lignin deposition correlates with root growth restriction under salt stress (Fig. 3b, c). An alternative, non-exclusive possibility is that PRX induction is largely secondary to upstream ROS and/or cell-wall integrity signaling; nevertheless, the ability of *PRX33/PRX71* overexpression to recapitulate lignification patterns (Fig. 2a) supports the idea that increased PRX activity is sufficient to drive lignin deposition under non-stress conditions (Fig. 2a). Together, these results support a functional link between elevated *PRX33/PRX71* activity and lignin deposition, even if the initiating signal in *gcn5* involves broader ROS and/or cell-wall integrity pathways.

While GCN5 is widely recognized for its role in histone acetylation, recent work in *Arabidopsis* has shown that it can also contribute to gene repression by acetylating the co-repressor TOPLESS. This acetylation promotes TOPLESS interaction with the NOVEL INTERACTOR OF JAZ (NINJA) protein and its recruitment to target promoters, resulting in chromatin compaction and transcriptional repression, including repression of jasmonate- responsive genes (An et al., 2022). In our study, reduced H3K9ac enrichment at the *PRX71* and *PRX33* promoter regions in the *gcn5* mutant argues against a simple model in which *GCN5* directly activates these PRX loci (Fig. 4a, b). Instead, our findings suggest that *GCN5* indirectly regulates *PRX33* and *PRX71*, potentially through transcription factors such as *MYBS2* and *GATA21* (Fig. 4d,e; Fig. S3a,b). This model is consistent with our observation that H3K9ac is reduced at PRX promoters (Fig. 4a,b) while *PRX33/PRX71* transcript abundance is elevated (Fig. 1b), implying an indirect regulatory route rather than direct activation. Evidence from rice supports a repressive role for *MYBS2*, as reduced *MYBS2* expression leads to elevated *αAmy* gene induction under abiotic stress conditions and improved stress tolerance (Chen et al., 2019). Together, these observations support a working model in which GCN5 maintains an acetylation-dependent transcriptional program that supports expression of PRX-constraining TFs, thereby constraining *PRX33/PRX71* expression and limiting stress-associated lignification and its growth trade-offs under salt stress (Fig. 4 model). In the absence of GCN5, reduced H3K9ac at TF loci may lower TF abundance, relieving repression on *PRX33/PRX71* and promoting lignin deposition. This regulatory logic is summarized in Figure 5. In wild type, GCN5 promotes H3K9ac at loci encoding PRX-regulating transcription factors (e.g., MYBS2 and GATA21), maintaining their expression. These TFs repress PRX33/PRX71, thereby limiting PRX-driven lignin deposition. In the

gcn5 mutant, reduced H3K9ac is associated with decreased TF expression, relieving repression of PRX33/PRX71 and resulting in elevated PRX activity and enhanced lignin deposition (Fig. 5). This model provides a coherent explanation for the apparent disconnect between reduced H3K9ac at PRX promoters (Fig. 4a,b) and increased PRX33/PRX71 transcript abundance (Fig. 1b), and it is consistent with the ability of PRX33/PRX71 overexpression to drive lignification under non-stress conditions (Fig. 2a) and with reduced salt-associated lignin deposition in *prx* mutants (Fig. 3d).

Future experiments that directly test causality, for example, genetic epistasis between *gcn5* and *prx33/prx71*, quantitative ROS and lignin measurements beyond staining, and functional validation of MYBS2/GATA21 at PRX promoters, will be important to distinguish primary chromatin-mediated effects from downstream stress responses and to refine the regulatory hierarchy. More broadly, these approaches will help clarify whether *PRX33/PRX71* act as key effectors of the *gcn5* phenotype or primarily reflect downstream remodeling of ROS and cell-wall integrity signaling under salt stress.

Material and Methods

Plant material and growth conditions

Arabidopsis thaliana T-DNA insertion lines *gcn5* (*SALK_048427*), *prx71-1* (*SALK_123643C*), *prx71-2* (*SALK_121202C*), and *prx33* (*SALK_062314C*) were obtained from the Nottingham Arabidopsis Stock Centre (NASC). All mutants are in the Columbia-0 (Col-0) background, and Col-0 was used as the wild-type control for all experiments.

Seeds were surface sterilized in 70% (v/v) ethanol containing 0.02% (v/v) Triton X-100 for 5 min, followed by 1 min in 96% (v/v) ethanol and five rinses in sterile water. Seeds were plated on half-strength Murashige and Skoog (MS) medium (Duchefa, M0222.0050) adjusted to pH 5.8 and supplemented with 0.8% (w/v) agar and 0.05% (w/v) MES unless stated otherwise. After 2 days of stratification in the dark at 4 °C, plates were transferred to a growth chamber maintained at 22 °C under a 16 h light/8 h dark photoperiod (light intensity 128.26 μmol m□2 s□1). All treatments were performed using sodium chloride and isoxaben, unless otherwise indicated.

Plasmid construction and plant transformation

PRX71 and *PRX33* overexpression constructs were generated using MultiSite Gateway cloning (Invitrogen; Thermo Fisher Scientific). The coding sequences (CDS) of PRX71 (984 bp) and PRX33 (1,062 bp) were amplified from Arabidopsis cDNA using gene-specific primers (Supplementary Table S1). PCR products were recombined into pDONR221 using BP Clonase II enzyme mix (Invitrogen), yielding entry clones carrying PRX71 or PRX33 CDS.

For expression in plants, an LR recombination reaction was performed using LR Clonase II Plus enzyme mix (Invitrogen) to assemble the CaMV 35S promoter, an mVenus YFP tag, and the PRX CDS fragments into the destination vector pBm43GW (Karimi et al., 2007)). The resulting constructs (35S::PRX71-YFP and 35S::PRX33-YFP) were introduced into Agrobacterium tumefaciens strain

GV3101 (pSoup) (Lifeasible) and transformed into Col-0 plants by floral dip. T1 plants were used for all subsequent experiments. All primers are listed in Supplementary Table S2.

Histochemical detection of ROS accumulation

Reactive oxygen species accumulation was assessed using 3,3′-diaminobenzidine (DAB) staining. Ten-day-old seedlings were treated with 0 mM or 150 mM NaCl on half-strength MS medium for 6 h. Seedlings were then infiltrated with 0.1% (w/v) DAB dissolved in 10 mM MES buffer (pH 6.5) until fully saturated and incubated for 40 min under light. After staining, seedlings were rinsed with water and chlorophyll was removed by incubation in 100% ethanol overnight. Samples were stored in water until imaging. Images were acquired using an Olympus SZ16 stereomicroscope equipped with a PROMICAM 2-5CP digital camera.

Histochemical detection of lignin deposition

Lignin deposition in roots was assessed by phloroglucinol–HCl staining. Seedlings were treated with 0 mM or 150 mM NaCl on half-strength MS medium for 6 h. Roots were stained with 1% (w/v) phloroglucinol–HCl (Pradhan Mitra & Loqué, 2014) for 10 min at room temperature. Stained samples were imaged immediately using an Olympus MacroView MVX10 stereomicroscope.

Physiological assays

Root growth assays

For root length measurements, seedlings were grown vertically on half-strength MS medium for 5 days and then transferred to one of the following media: control (0 mM NaCl), 150 mM NaCl, or 2.5 nM isoxaben. Plates were returned to vertical orientation, and seedlings were grown for an additional 7 days. Primary root lengths were measured at the endpoint (day 12). Each treatment was performed using at least three independent biological replicates.

Survival rate analysis

For salt survival assays, 5-day-old seedlings were transferred to half-strength MS medium containing 0 mM or 150 mM NaCl and grown for 7 days. Survival was determined as the percentage of seedlings that remained green and viable relative to the total number of transferred seedlings. Each treatment included at least three biological replicates.

RNA extraction and quantitative real-time PCR (qRT–PCR)

For gene expression analyses, seedlings were grown on half-strength MS medium (pH 5.8) without sucrose for 10 days. Salt treatments were performed by transferring seedlings to liquid MS medium containing 150 mM NaCl, and tissue was harvested at 0, 3, 6, and 12 h after treatment. Samples were immediately frozen in liquid nitrogen and homogenized with glass beads using a bead mill.

Total RNA was extracted using ROTI®ZOL (Karl Roth, 9319.2) according to the manufacturer's instructions, following the workflow described by (Colina et al., 2026). RNA was treated with DNase I to remove genomic DNA contamination as described by (Colina et al., 2026). First-strand cDNA was synthesized from 1 µg DNase-treated RNA using the RevertAid cDNA Synthesis Kit (Thermo Fisher Scientific, K1621).

Quantitative real-time PCR was performed using gene-specific primers (Supplementary Table S1). Expression was normalized to the housekeeping gene [PP2AA3], following Czechowski et al. (2005). Relative expression levels were calculated using the ΔΔCT method. Each condition was measured using three independent biological replicates and two technical replicates per biological replicate.

Chromatin immunoprecipitation (ChIP) and ChIP–qPCR

ChIP was performed using a crosslinked Arabidopsis ChIP protocol adapted from the Iva lab method (Mozgová et al., 2015). Wild-type (Col-0) and *gcn5* seedlings were grown on half-strength MS plates for 10 days and treated in liquid half-strength MS with 150 mM NaCl for 3 h; control samples were mock-treated without NaCl. Tissue (~100 mg) was crosslinked in 1% formaldehyde by vacuum infiltration (10 min) and quenched with 0.125 M glycine (5 min). Samples were washed, snap-frozen, and ground in liquid nitrogen. Nuclei were extracted in Modified Extraction Buffer, filtered through Miracloth, and pelleted (1500 rcf, 10 min, 4 °C). Chromatin was lysed in 1% SDS and sonicated (7 cycles, 30 s ON/30 s OFF, high power) to obtain ~0.3–1.5 kb fragments, then diluted with ChIP dilution buffer to reduce SDS to 0.1% and clarified by centrifugation. Ten percent of each sample was saved as input DNA. Immunoprecipitation was performed overnight at 4 °C with rotation using anti-H3K9ac and, where indicated, total H3, or normal IgG as a negative control. Immune complexes were captured with Protein A agarose beads and washed using low- and high-salt wash buffers. Chromatin was eluted twice (elution buffer; 65 °C, 15 min) and crosslinks were reversed by NaCl addition and incubation at 65 °C for ≥6 h. Samples were treated with proteinase K (45 °C, 1 h), and DNA was purified using the kit.

ChIP enrichment was quantified by qPCR using primers targeting promoter regions (ADD Supplementary Table ID), with two technical replicates per biological replicate. Enrichment was calculated relative to input DNA and normalized to total H3. A transposable element locus (*At4g03770*) was used as a negative control. All primers are listed in Supplementary Table S1.

Statistical analysis

All statistical analyses were performed in R (2023-12-1; Build 402; Posit Software) using RStudio (2024-04-24, 4.4.0; R Foundation). Data were initially tested for normality and homogeneity of variances. Levene's test and F-test were applied to assess variance homogeneity. For datasets meeting parametric assumptions, t-tests, and two-way ANOVA were used, with Tukey's post-hoc test applied

for multiple pairwise comparisons. For datasets that did not meet parametric assumptions, Kruskal–Wallis tests were used as a non-parametric alternative followed by wilcoxon post-hoc test for pairwise comparisons. In all analyses, $p < 0.05$ was considered significant.

Acknowledgements

This work was supported by the Czech Science Foundation grants nr. 22-17092S (PK and MW). We thank Dr. Fatemeh Aflaki for help with Chip-qPCR and Growth Facility (Jan Kadlec), BC Core Facilities, Institute for Plant Molecular Biology, Biology Centre CAS.

Competing interests

The authors declare no competing interests.

Author contributions

MS, PK, IM and MW conceived the study and designed the research. MS and JM carried out the work. MS, JM, PK, IM and MW analyzed the data. MS wrote the first draft. All authors edited the final draft of the paper. PK and MW acquired funding for the research.

Data availability

Data, plasmids and transgenic plant seeds generated for this study are available upon request from Michael Wrzaczek.

References

An, C., Deng, L., Zhai, H., You, Y., Wu, F., Zhai, Q., Goossens, A., & Li, C. (2022). Regulation of jasmonate signaling by reversible acetylation of TOPLESS in Arabidopsis. *Molecular Plant*, *15*(8), 1329–1346. https://doi.org/10.1016/j.molp.2022.06.014

Baxter, A., Mittler, R., & Suzuki, N. (2014). ROS as key players in plant stress signalling. *Journal of Experimental Botany*, *65*(5), 1229–1240. https://doi.org/10.1093/jxb/ert375

Benhamed, M., Bertrand, C., Servet, C., & Zhou, D.-X. (2006). *Arabidopsis GCN5* , *HD1* , and *TAF1/HAF2* Interact to Regulate Histone Acetylation Required for Light-Responsive Gene Expression. *The Plant Cell*, *18*(11), 2893–2903. https://doi.org/10.1105/tpc.106.043489

Benhamed, M., Martin□Magniette, M., Taconnat, L., Bitton, F., Servet, C., De Clercq, R., De Meyer, B., Buysschaert, C., Rombauts, S., Villarroel, R., Aubourg, S., Beynon, J., Bhalerao, R. P., Coupland, G., Gruissem, W., Menke, F. L. H., Weisshaar, B., Renou, J., Zhou, D., & Hilson, P. (2008). Genome□scale Arabidopsis promoter array identifies targets of the histone acetyltransferase GCN5. *The Plant Journal*, *56*(3), 493–504. https://doi.org/10.1111/j.1365-313X.2008.03606.x

Bischoff, V., Cookson, S. J., Wu, S., & Scheible, W.-R. (2009). Thaxtomin A affects CESA-complex density, expression of cell wall genes, cell wall composition, and causes ectopic lignification in Arabidopsis thaliana seedlings. *Journal of Experimental Botany*, *60*(3), 955–965. https://doi.org/10.1093/jxb/ern344

Boudsocq, M., & Sheen, J. (2013). CDPKs in immune and stress signaling. *Trends in Plant Science*, *18*(1), 30–40. https://doi.org/10.1016/j.tplants.2012.08.008

Boyce, C. K., Zwieniecki, M. A., Cody, G. D., Jacobsen, C., Wirick, S., Knoll, A. H., & Holbrook, N. M. (2004). Evolution of xylem lignification and hydrogel transport regulation. *Proceedings of the National Academy of Sciences*, *101*(50), 17555–17558. https://doi.org/10.1073/pnas.0408024101

Caño□Delgado, A., Penfield, S., Smith, C., Catley, M., & Bevan, M. (2003). Reduced cellulose synthesis invokes lignification and defense responses in *Arabidopsis thaliana*. *The Plant Journal*, *34*(3), 351–362. https://doi.org/10.1046/j.1365-313X.2003.01729.x

Chen, Y.-S., David Ho, T.-H., Liu, L., Lee, D. H., Lee, C.-H., Chen, Y.-R., Lin, S.-Y., Lu, C.-A., & Yu, S.-M. (2019). Sugar starvation-regulated MYBS2 and 14-3-3 protein interactions enhance plant growth, stress tolerance, and grain weight in rice. *Proceedings of the National Academy of Sciences*, *116*(43), 21925–21935. https://doi.org/10.1073/pnas.1904818116

Chow, C.-N., Yang, C.-W., Wu, N.-Y., Wang, H.-T., Tseng, K.-C., Chiu, Y.-H., Lee, T.-Y., & Chang, W.-C. (2024). PlantPAN 4.0: Updated database for identifying conserved non-coding sequences and exploring dynamic transcriptional regulation in plant promoters. *Nucleic Acids Research*, *52*(D1), D1569–D1578. https://doi.org/10.1093/nar/gkad945

Chun, H. J., Baek, D., Cho, H. M., Lee, S. H., Jin, B. J., Yun, D.-J., Hong, Y.-S., & Kim, M. C. (2019). Lignin biosynthesis genes play critical roles in the adaptation of *Arabidopsis* plants to high-salt stress. *Plant Signaling & Behavior*, *14*(8), 1625697. https://doi.org/10.1080/15592324.2019.1625697

Colina, F. J., Krasensky□Wrzaczek, J., Pérez□Guillén, A., & Wrzaczek, M. (2026). CRK2 modulates flowering in Arabidopsis together with GLYCINE□RICH RNA □ BINDING PROTEIN 7. *New Phytologist*, nph.70901. https://doi.org/10.1111/nph.70901

Cosgrove, D. J. (2005). Growth of the plant cell wall. *Nature Reviews Molecular Cell Biology*, *6*(11), 850–861. https://doi.org/10.1038/nrm1746

Cosgrove, D. J. (2016). Plant cell wall extensibility: Connecting plant cell growth with cell wall structure, mechanics, and the action of wall-modifying enzymes. *Journal of Experimental Botany*, *67*(2), 463–476. https://doi.org/10.1093/jxb/erv511

Cosio, C., & Dunand, C. (2009). Specific functions of individual class III peroxidase genes. *Journal of Experimental Botany*, *60*(2), 391–408. https://doi.org/10.1093/jxb/ern318

Daudi, A., Cheng, Z., O'Brien, J. A., Mammarella, N., Khan, S., Ausubel, F. M., & Bolwell, G. P. (2012). The Apoplastic Oxidative Burst Peroxidase in *Arabidopsis* Is a Major Component of Pattern-Triggered Immunity. *The Plant Cell*, *24*(1), 275–287. https://doi.org/10.1105/tpc.111.093039

Davidson, R. S., Choudhury, H., Origgi, S., Castellan, A., Trichet, V., & Capretti, G. (1995). The reaction of phloroglucinol in the presence of acid with lignin-containing materials. *Journal of Photochemistry and Photobiology A: Chemistry*, *91*(1), 87–93. https://doi.org/10.1016/1010-6030(95)04101-K

De Smet, B., Yang, X., Plskova, Z., Castell, C., Fernández-Fernández, A., Dard, A., Masood, J., Mhamdi, A., Huang, J., Vertommen, D., Chan, K. X., Pyr Dit Ruys, S., Messens, J., Kerchev, P. I., & Van Breusegem, F. (2025). The nuclear sulfenome of Arabidopsis: Spotlight on histone acetyltransferase GCN5 regulation through functional thiols. *Journal of Experimental Botany*, *76*(6), 1569–1584. https://doi.org/10.1093/jxb/erae514

Denness, L., McKenna, J. F., Segonzac, C., Wormit, A., Madhou, P., Bennett, M., Mansfield, J., Zipfel, C., & Hamann, T. (2011). Cell Wall Damage-Induced Lignin Biosynthesis Is Regulated by a Reactive Oxygen Species- and Jasmonic Acid-Dependent Process in Arabidopsis. *Plant Physiology*, *156*(3), 1364–1374. https://doi.org/10.1104/pp.111.175737

Ding, Y., Fromm, M., & Avramova, Z. (2012). Multiple exposures to drought "train" transcriptional responses in Arabidopsis. *Nature Communications*, *3*(1), 740. https://doi.org/10.1038/ncomms1732

Gutierrez, R., Lindeboom, J. J., Paredez, A. R., Emons, A. M. C., & Ehrhardt, D. W. (2009). Arabidopsis cortical microtubules position cellulose synthase delivery to the plasma membrane and interact with cellulose synthase trafficking compartments. *Nature Cell Biology*, *11*(7), 797–806. https://doi.org/10.1038/ncb1886

Hamann, T. (2015). The Plant Cell Wall Integrity Maintenance Mechanism—Concepts for Organization and Mode of Action. *Plant and Cell Physiology*, *56*(2), 215–223. https://doi.org/10.1093/pcp/pcu164

Hu, Z., Song, N., Zheng, M., Liu, X., Liu, Z., Xing, J., Ma, J., Guo, W., Yao, Y., Peng, H., Xin, M., Zhou, D., Ni, Z., & Sun, Q. (2015). Histone acetyltransferase GCN 5 is essential for heat stress responsive gene activation and thermotolerance in Arabidopsis. *The Plant Journal*, *84*(6), 1178–1191. https://doi.org/10.1111/tpj.13076

Jalmi, S. K., & Sinha, A. K. (2015). ROS mediated MAPK signaling in abiotic and biotic stress-striking similarities and differences. *Frontiers in Plant Science*, *6*. https://doi.org/10.3389/fpls.2015.00769

Karimi, M., Bleys, A., Vanderhaeghen, R., & Hilson, P. (2007). Building Blocks for Plant Gene Assembly. *Plant Physiology*, *145*(4), 1183–1191. https://doi.org/10.1104/pp.107.110411

Kim, S., Piquerez, S. J. M., Ramirez-Prado, J. S., Mastorakis, E., Veluchamy, A., Latrasse, D., Manza-Mianza, D., Brik-Chaouche, R., Huang, Y., Rodriguez-Granados, N. Y., Concia, L., Blein, T., Citerne, S., Bendahmane, A., Bergounioux, C., Crespi, M., Mahfouz, M. M., Raynaud, C., Hirt, H., … Benhamed, M. (2020). GCN5 modulates salicylic acid homeostasis by regulating H3K14ac levels at the 5′ and 3′ ends of its target genes. *Nucleic Acids Research*, *48*(11), 5953–5966. https://doi.org/10.1093/nar/gkaa369

Kornet, N., & Scheres, B. (2009). Members of the GCN5 Histone Acetyltransferase Complex Regulate PLETHORA-Mediated Root Stem Cell Niche Maintenance and Transit Amplifying Cell Proliferation in *Arabidopsis*. *The Plant Cell*, *21*(4), 1070–1079. https://doi.org/10.1105/tpc.108.065300

Lämke, J., & Bäurle, I. (2017). Epigenetic and chromatin-based mechanisms in environmental stress adaptation and stress memory in plants. *Genome Biology*, *18*(1), 124. https://doi.org/10.1186/s13059-017-1263-6

Ma, L., Xing, L., Li, Z., & Jiang, D. (2025). Epigenetic control of plant abiotic stress responses. *Journal of Genetics and Genomics*, *52*(2), 129–144. https://doi.org/10.1016/j.jgg.2024.09.008

Marjamaa, K., Kukkola, E. M., & Fagerstedt, K. V. (2009). The role of xylem class III peroxidases in lignification. *Journal of Experimental Botany*, *60*(2), 367–376. https://doi.org/10.1093/jxb/ern278

Mittler, R. (2002). Oxidative stress, antioxidants and stress tolerance. *Trends in Plant Science*, *7*(9), 405–410. https://doi.org/10.1016/S1360-1385(02)02312-9

Moraga, F., & Aquea, F. (2015). Composition of the SAGA complex in plants and its role in controlling gene expression in response to abiotic stresses. *Frontiers in Plant Science*, *6*. https://doi.org/10.3389/fpls.2015.00865

Moura, J. C. M. S., Bonine, C. A. V., De Oliveira Fernandes Viana, J., Dornelas, M. C., & Mazzafera, P. (2010). Abiotic and Biotic Stresses and Changes in the Lignin Content and Composition in Plants. *Journal of Integrative Plant Biology*, *52*(4), 360–376. https://doi.org/10.1111/j.1744-7909.2010.00892.x

Mozgová, I., Wildhaber, T., Liu, Q., Abou-Mansour, E., L'Haridon, F., Métraux, J.-P., Gruissem, W., Hofius, D., & Hennig, L. (2015). Chromatin assembly factor CAF-1 represses priming of plant defence response genes. *Nature Plants*, *1*(9), 15127. https://doi.org/10.1038/nplants.2015.127

O'Brien, J. A., Daudi, A., Finch, P., Butt, V. S., Whitelegge, J. P., Souda, P., Ausubel, F. M., & Bolwell, G. P. (2012). A Peroxidase-Dependent Apoplastic Oxidative Burst in Cultured Arabidopsis Cells Functions in MAMP-Elicited Defense. *Plant Physiology*, *158*(4), 2013–2027. https://doi.org/10.1104/pp.111.190140

Oliveira, D. M., Mota, T. R., Salatta, F. V., Sinzker, R. C., Končitíková, R., Kopečný, D., Simister, R., Silva, M., Goeminne, G., Morreel, K., Rencoret, J., Gutiérrez, A., Tryfona, T., Marchiosi, R., Dupree, P., Del Río, J. C., Boerjan, W., McQueen□Mason, S. J., Gomez, L. D., … Dos Santos, W. D. (2020). Cell wall remodeling under salt stress: Insights into changes in polysaccharides, feruloylation, lignification, and phenolic metabolism in maize. *Plant, Cell & Environment*, *43*(9), 2172–2191. https://doi.org/10.1111/pce.13805

Passardi, F., Penel, C., & Dunand, C. (2004). Performing the paradoxical: How plant peroxidases modify the cell wall. *Trends in Plant Science*, *9*(11), 534–540. https://doi.org/10.1016/j.tplants.2004.09.002

Pedreira, J., Herrera, M. T., Zarra, I., & Revilla, G. (2011). The overexpression of *AtPrx37* , an apoplastic peroxidase, reduces growth in *Arabidopsis*. *Physiologia Plantarum*, *141*(2), 177–187. https://doi.org/10.1111/j.1399-3054.2010.01427.x

Persson, S., Paredez, A., Carroll, A., Palsdottir, H., Doblin, M., Poindexter, P., Khitrov, N., Auer, M., & Somerville, C. R. (2007). Genetic evidence for three unique components in primary cell-wall cellulose synthase complexes in *Arabidopsis*. *Proceedings of the National Academy of Sciences*, *104*(39), 15566–15571. https://doi.org/10.1073/pnas.0706592104

Pradhan Mitra, P., & Loqué, D. (2014). Histochemical Staining of Arabidopsis thaliana Secondary Cell Wall Elements. *Journal of Visualized Experiments*, *87*, 51381. https://doi.org/10.3791/51381

Raggi, S., Ferrarini, A., Delledonne, M., Dunand, C., Ranocha, P., Lorenzo, G. D., Cervone, F., & Ferrari, S. (2015). *The Arabidopsis Class III Peroxidase AtPRX71 Negatively Regulates Growth under Physiological Conditions and in Response to Cell Wall Damage1[OPEN]*. *169*.

Rogers, L. A., & Campbell, M. M. (2004). The genetic control of lignin deposition during plant growth and development. *New Phytologist*, *164*(1), 17–30. https://doi.org/10.1111/j.1469-8137.2004.01143.x

Sako, K., Kim, J.-M., Matsui, A., Nakamura, K., Tanaka, M., Kobayashi, M., Saito, K., Nishino, N., Kusano, M., Taji, T., Yoshida, M., & Seki, M. (2016). Ky-2, a Histone Deacetylase Inhibitor, Enhances High-Salinity Stress Tolerance in *Arabidopsis thaliana*. *Plant and Cell Physiology*, *57*(4), 776–783. https://doi.org/10.1093/pcp/pcv199

Scheible, W.-R., Eshed, R., Richmond, T., Delmer, D., & Somerville, C. (2001). Modifications of cellulose synthase confer resistance to isoxaben and thiazolidinone herbicides in *Arabidopsis Ixr1* mutants. *Proceedings of the National Academy of Sciences*, *98*(18), 10079–10084. https://doi.org/10.1073/pnas.191361598

Servet, C., Conde E Silva, N., & Zhou, D.-X. (2010). Histone Acetyltransferase AtGCN5/HAG1 Is a Versatile Regulator of Developmental and Inducible Gene Expression in Arabidopsis. *Molecular Plant*, *3*(4), 670–677. https://doi.org/10.1093/mp/ssq018

Shigeto, J., Kiyonaga, Y., Fujita, K., Kondo, R., & Tsutsumi, Y. (2013). Putative Cationic Cell-Wall-Bound Peroxidase Homologues in Arabidopsis, AtPrx2, AtPrx25, and AtPrx71, Are Involved in Lignification. *Journal of Agricultural and Food Chemistry*, *61*(16), 3781–3788. https://doi.org/10.1021/jf400426g

Tenhaken, R. (2015). Cell wall remodeling under abiotic stress. *Frontiers in Plant Science*, *5*. https://doi.org/10.3389/fpls.2014.00771

Ueda, M., & Seki, M. (2020). Histone Modifications Form Epigenetic Regulatory Networks to Regulate Abiotic Stress Response. *Plant Physiology*, *182*(1), 15–26. https://doi.org/10.1104/pp.19.00988

Vlachonasios, K. E., Thomashow, M. F., & Triezenberg, S. J. (2003). Disruption Mutations of *ADA2b* and *GCN5* Transcriptional Adaptor Genes Dramatically Affect Arabidopsis Growth, Development, and Gene Expression[W]. *The Plant Cell*, *15*(3), 626–638. https://doi.org/10.1105/tpc.007922

Wu, C.-J., Yuan, D.-Y., Liu, Z.-Z., Xu, X., Wei, L., Cai, X.-W., Su, Y.-N., Li, L., Chen, S., & He, X.-J. (2023). Conserved and plant-specific histone acetyltransferase complexes cooperate to regulate gene transcription and plant development. *Nature Plants*, *9*(3), 442–459. https://doi.org/10.1038/s41477-023-01359-3

Wurzinger, B., Mair, A., Pfister, B., & Teige, M. (2011). Cross-talk of calcium-dependent protein kinase and MAP kinase signaling. *Plant Signaling & Behavior*, *6*(1), 8–12. https://doi.org/10.4161/psb.6.1.14012

Xia, X.-J., Zhou, Y.-H., Shi, K., Zhou, J., Foyer, C. H., & Yu, J.-Q. (2015). Interplay between reactive oxygen species and hormones in the control of plant development and stress tolerance. *Journal of Experimental Botany*, *66*(10), 2839–2856. https://doi.org/10.1093/jxb/erv089

Zheng, M., Lin, J., Liu, X., Chu, W., Li, J., Gao, Y., An, K., Song, W., Xin, M., Yao, Y., Peng, H., Ni, Z., Sun, Q., & Hu, Z. (2021a). Histone acetyltransferase TaHAG1 acts as a crucial regulator to strengthen salt tolerance of hexaploid wheat. *Plant Physiology*, *186*(4), 1951–1969. https://doi.org/10.1093/plphys/kiab187

Zheng, M., Lin, J., Liu, X., Chu, W., Li, J., Gao, Y., An, K., Song, W., Xin, M., Yao, Y., Peng, H., Ni, Z., Sun, Q., & Hu, Z. (2021b). Histone acetyltransferase TaHAG1 acts as a crucial regulator to strengthen salt tolerance of hexaploid wheat. *Plant Physiology*, *186*(4), 1951–1969. https://doi.org/10.1093/plphys/kiab187

Zheng, M., Liu, X., Lin, J., Liu, X., Wang, Z., Xin, M., Yao, Y., Peng, H., Zhou, D., Ni, Z., Sun, Q., & Hu, Z. (2019). Histone acetyltransferase GCN 5 contributes to cell wall integrity and salt stress tolerance by altering the expression of cellulose synthesis genes. *The Plant Journal*, *97*(3), 587–602. https://doi.org/10.1111/tpj.14144

Figure legends:

Figure 1. Enhanced ROS accumulation and upregulation of PRX genes in the *gcn5* mutant. (a) DAB staining of 10-day-old wild-type and *gcn5* seedlings after 6 h of treatment under control conditions, 150 mM NaCl, or with 300 nM isoxaben. Images are representative of at least three independent biological experiments. Scale bar = 0.5 mm. (b) Expression levels of selected PRX genes at different time points during 150 mM NaCl treatment. Transcript levels were normalized to a housekeeping gene and expressed relative to wild type at 0 h (=1). Data represent mean ± SE of three biological replicates. Statistical significance was determined using two-way ANOVA followed by Tukey's HSD test. Different letters indicate significant differences.

Figure 2. PRX33 and PRX71 contribute to lignin deposition. (a) Lignin deposition in roots of wild type, *gcn5* mutant, *prx71* mutant, *prx33* mutant, and 35S::PRX33 and 35S::PRX71 overexpression lines under control conditions. Black arrows indicate ectopic lignin deposition. Images are representative of at least three independent biological experiments. Scale bar = 50 μm.

Figure 3. Salt stress responses and lignin deposition. (a) Survival rates under salt stress. Survival was calculated relative to plants grown under control conditions. Data represent mean ± SE ($n \geq 3$ biological replicates). Statistical analysis was performed using two-way ANOVA after confirming homogeneity of variance (Levene's test, $p = 0.070$), followed by Tukey's HSD test. Different letters indicate significant differences.

(b) Root length was calculated relative to plants grown under control conditions. Primary root length (%) measured at day 12 for seedlings grown on control or 150 mM NaCl-containing medium. (c) Primary root length (%) measured at day 12 for seedlings grown on control or 2.5 nM isoxaben-containing medium. Root length was calculated relative to plants grown under control conditions. Data in (b) and (c) were analyzed using the Kruskal–Wallis test due to unequal variances (Levene's test, $p < 0.05$), followed by Wilcoxon post-hoc test. Different letters indicate significant differences.

(d) Lignin deposition in roots of wild type, *gcn5*, *prx71*, and *prx33* mutants after 6 h of 150 mM NaCl treatment. Arrows indicate ectopic lignin deposition in the *gcn5* mutant. Images are representative of at least three independent experiments. Scale bar = 50 μm.

Figure 4. GCN5 indirectly regulates PRX33 and PRX71 through chromatin modification and transcription factor activity. (a,b) ChIP–qPCR analysis of H3K9ac enrichment at the promoter regions of PRX71 (a) and PRX33 (b) in wild type and gcn5 seedlings under control and 150 mM NaCl conditions. ChIP was performed using anti-H3K9ac antibodies, and enrichment was normalized to total H3. Statistical analysis was performed using two-way ANOVA after confirming homogeneity of variance (Levene's test, $p > 0.05$), followed by Tukey's HSD test. (c) ChIP–qPCR analysis of H3K9ac enrichment at a transposable element locus (At4g03770) used as a negative control.

Enrichment was normalized to total H3. Statistical analysis was performed using two-way ANOVA followed by Tukey's HSD test.

(d) Relative expression of candidate transcription factor genes in wild type and gcn5 seedlings under control conditions, measured by qRT–PCR. Statistical analysis was performed using a two-tailed Student's t-test. (e) ChIP–qPCR analysis of H3K9ac enrichment at the promoter regions of MYBS2 and GATA21 in wild type and gcn5 seedlings under control conditions. ChIP was performed using anti-H3K9ac antibodies, and enrichment was normalized to total H3. Statistical analysis was performed using a two-tailed Student's t-test.

Figure 5. Proposed model for indirect regulation of *PRX33/PRX71* and lignin deposition by GCN5.

In wild type (top), GCN5 promotes H3K9 acetylation (H3K9ac) at loci encoding PRX-regulating transcription factors (TFs; e.g., MYBS2 and GATA21), maintaining TF expression. These TFs repress PRX33/PRX71, thereby limiting PRX-driven lignin deposition. In the gcn5 mutant (bottom), reduced H3K9ac is associated with decreased TF expression, relieving repression of PRX33/PRX71 and resulting in elevated PRX activity and enhanced lignin deposition. Arrows indicate positive regulation, flat bars indicate repression, up/down arrows indicate increased/decreased levels, and red X symbols indicate loss of GCN5 function and disruption of regulatory steps.

Supplementary figure legends:

Supplementary Figure S1. Salt sensitivity and differentially expressed PRX genes in the *gcn5* mutant. (a) Survival rates of seedlings after salt treatment. Values are normalized to the corresponding genotype grown under control conditions. Data represent mean ± SE ($n \geq 3$ biological replicates). Statistical analysis was performed using two-way ANOVA after confirming homogeneity of variance (Levene's test, $p > 0.05$), followed by Tukey's HSD test. Different letters indicate significant differences. (b) Primary root length (mm) measured at day 12 for seedlings grown on control or 150 mM NaCl-containing medium. Statistical analysis was performed using the Kruskal–Wallis test due to unequal variances (Levene's test, $p < 0.05$), followed by Wilcoxon post-hoc test. Different letters indicate significant differences.

(c) Differentially expressed *PRX* genes in the *gcn5* mutant identified from transcriptomic analysis. (d) Expression levels of differentially expressed *PRX* genes at various time points during 150 mM NaCl treatment. Data represent mean ± SE of two biological replicates. Statistical significance was determined using two-way ANOVA followed by Tukey's HSD test. Different letters indicate significant differences.

Supplementary Figure S2. Salt stress responses in gcn5, complementation lines, and *prx* mutants. (a) Survival of plants grown on control and NaCl containing media. (b) Primary root length

(mm) measured at day 12 for seedlings grown on control or 150 mM NaCl-containing medium. Data were analyzed using the Kruskal–Wallis test due to unequal variances (Levene's test, $p < 0.05$), followed by Wilcoxon post-hoc test. Different letters indicate significant differences.

Supplementary Figure S3. Controls and candidate transcription factor analyses. (a) Expression levels of differentially expressed transcription factor genes under control conditions measured by qRT–PCR. Data represent mean ± SD of three biological replicates. Statistical significance was determined using a two-tailed Student's t-test. (b) ChIP–qPCR analysis of H3K9ac enrichment at the promoter regions of candidate transcription factor genes in wild type and gcn5 seedlings under control conditions. Enrichment was normalized to total H3. Statistical significance was determined using two-tailed Student's t-test.

Supplementary TableS1. Primer sequences used for Cloning, qRT-PCR, ChIP qRT-PCR analyses.

Supplementary TableS2. Potential transcription factors binding sites in the promoters of *PRX71* and *PRX33*

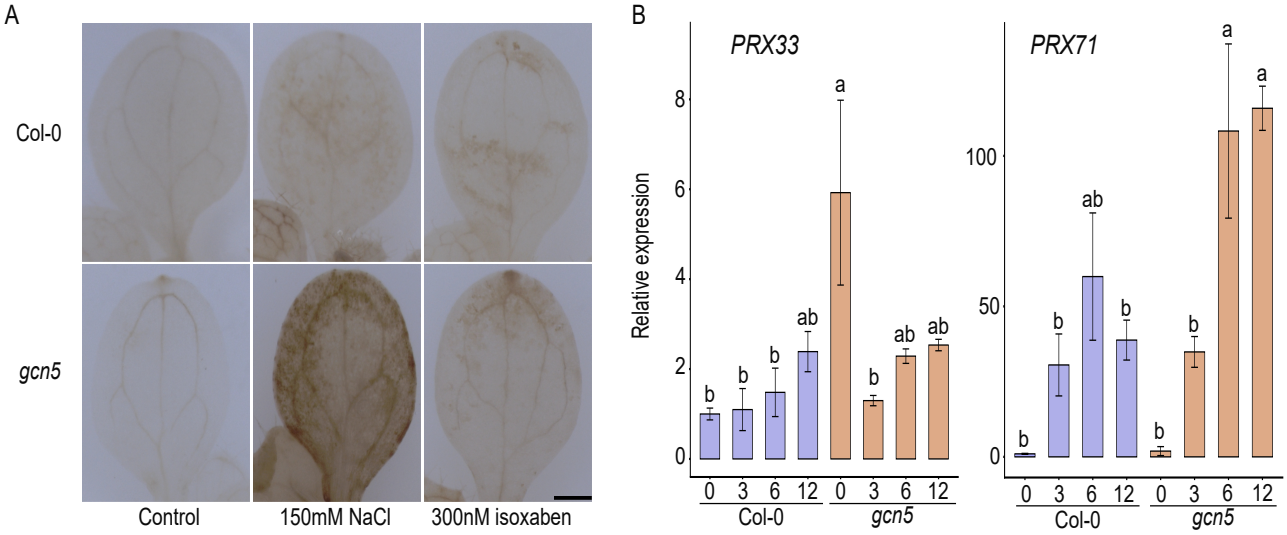
A
Col-0
gcn5
Control
150mM NaCl
300nM isoxaben
B
PRX33
PRX71
Relative expression
0
2
4
6
8
0
50
100
b
b
b
ab
a
b
ab
ab
b
ab
b
b
b
a
a
0 3 6 12 0 3 6 12
Col-0
gcn5

A

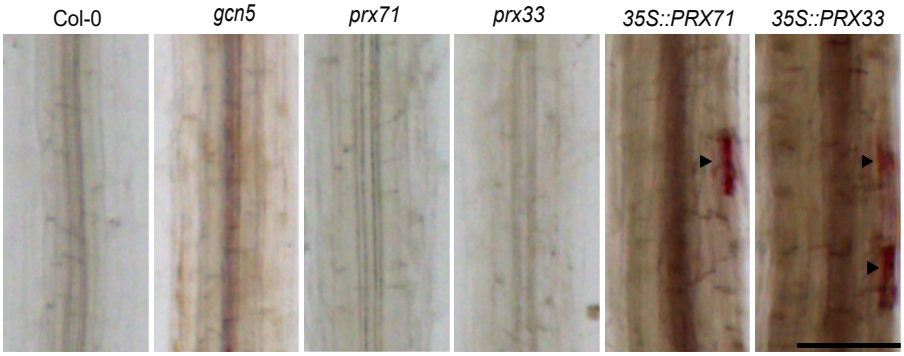

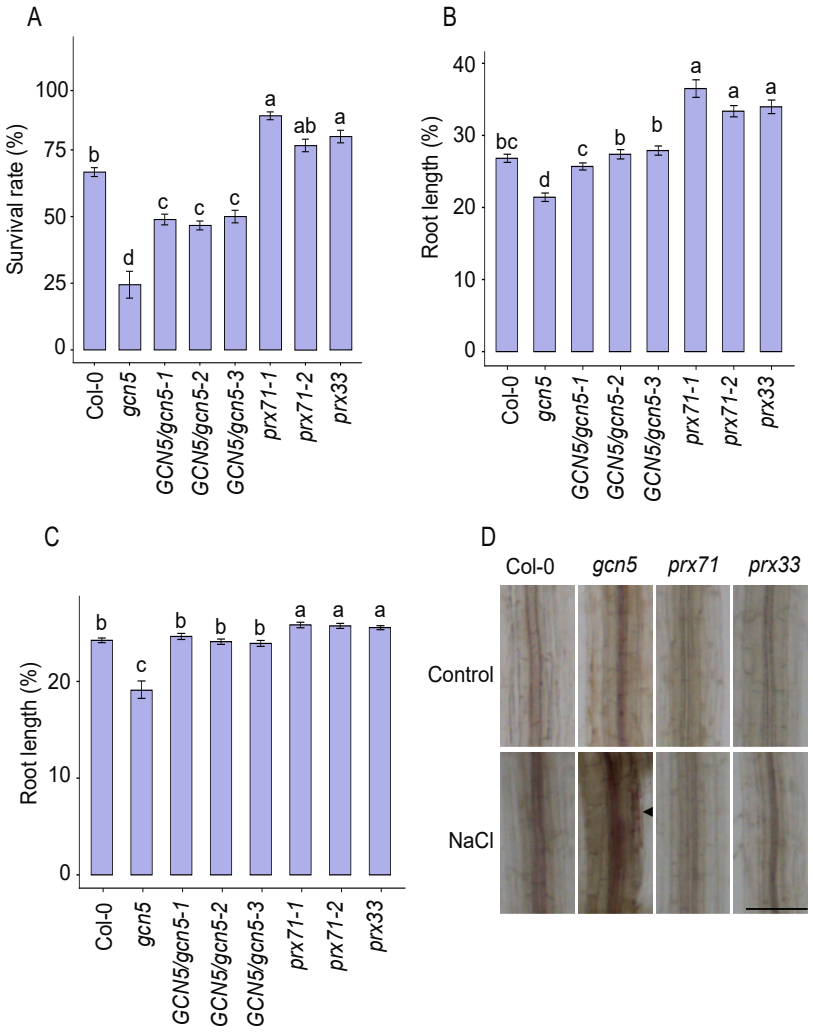
A
Survival rate (%)
0
25
50
75
100
b
d
c
c
c
a
ab
a
Col-0
gcn5
GCN5/gcn5-1
GCN5/gcn5-2
GCN5/gcn5-3
prx71-1
prx71-2
prx33
B
Root length (%)
0
10
20
30
40
bc
d
c
b
b
a
a
a
Col-0
gcn5
GCN5/gcn5-1
GCN5/gcn5-2
GCN5/gcn5-3
prx71-1
prx71-2
prx33
C
Root length (%)
0
10
20
b
c
b
b
b
a
a
a
Col-0
gcn5
GCN5/gcn5-1
GCN5/gcn5-2
GCN5/gcn5-3
prx71-1
prx71-2
prx33
D
Col-0
gcn5
prx71
prx33
Control
NaCl

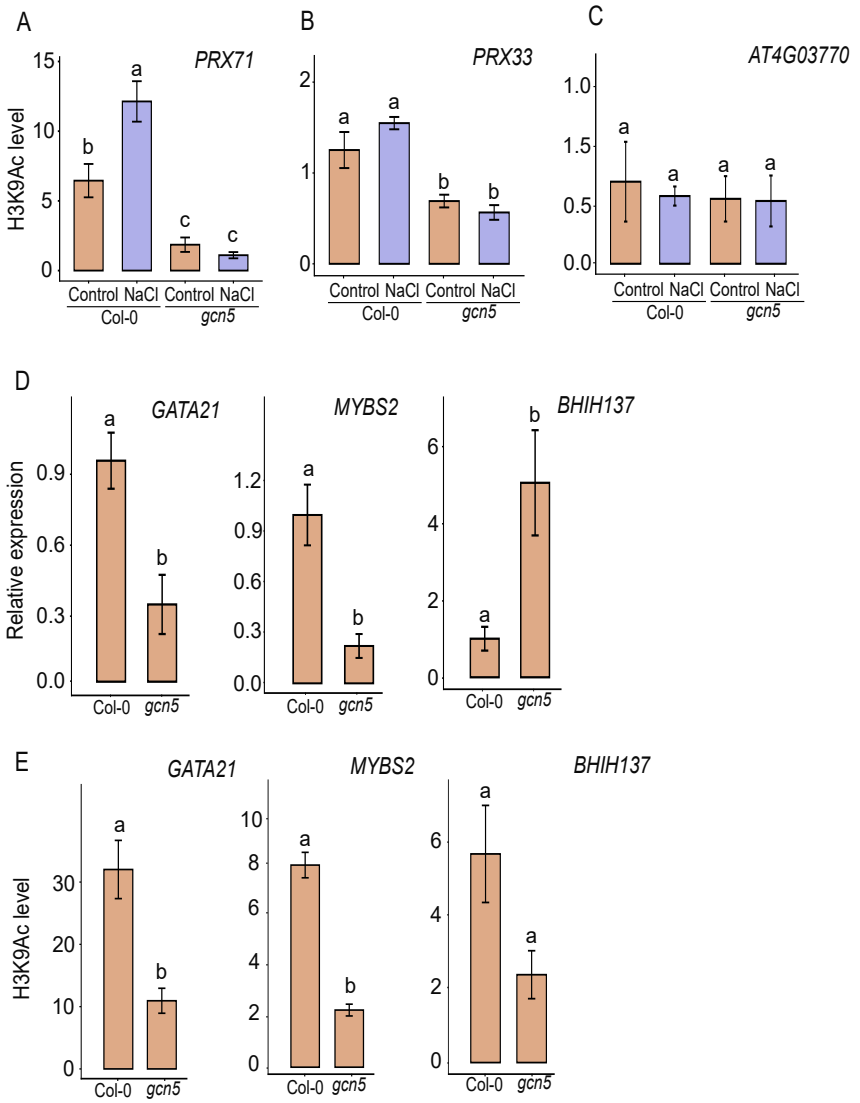
A
PRX71
H3K9Ac level
15
10
5
0
a
b
c
c
Control NaCl Control NaCl
Col-0
gcn5
B
PRX33
2
1
0
a
a
b
b
Control NaCl Control NaCl
Col-0
gcn5
C
AT4G03770
1.0
1.5
0.5
0.0
a
a
a
a
Control NaCl Control NaCl
Col-0
gcn5
D
GATA21
MYBS2
BHIH137
Relative expression
0.9
0.6
0.3
0.0
1.2
6
4
2
0
a
b
Col-0
gcn5
E
GATA21
MYBS2
BHIH137
H3K9Ac level
30
20
10
0
8
6
4
2
a
b
Col-0
gcn5